Supporting Information for

Twisted Non-diffracting Beams Through All Dielectric Meta-axicon

Nasir Mahmood,‡[a] Heonyeong Jeong,‡[d] Inki Kim,‡[d] Muhammad Qasim Mehmood,‡[b] Muhammad Zubair,[b] Ali Akbar,c Murtaza Saleem,[c] Muhammad Sabieh Anwar,*[c] Farooq Ahmad Tahir*[a] and Junsuk Rho*[d,e]

a. Research Institute for Microwave and Millimeter-wave Studies (RIMMS), National University of Sciences and Technology (NUST), Islamabad 44000, Pakistan. E-mail: farooq.tahir@seecs.edu.pk

b. Department of Electrical Engineering, Information Technology University of the Punjab, Lahore 54600, Pakistan

c. Laboratory for Quantum Technologies, Department of Physics, Syed Babar Ali School of Science and Engineering (SBASSE), Lahore University of Management Sciences (LUMS), Opposite Sector U, D.H.A. Lahore 54792, Pakistan. E-mail: sabieh@lums.edu.pk

d. Department of Mechanical Engineering, Pohang University of Science and Technology (POSTECH), Pohang 37673, Republic of Korea. E-mail: jsrho@postech.ac.kr

e. Department of Chemical Engineering, Pohang University of Science and Technology (POSTECH), Pohang 37673, Republic of Korea

‡These authors contributed equally to this work.

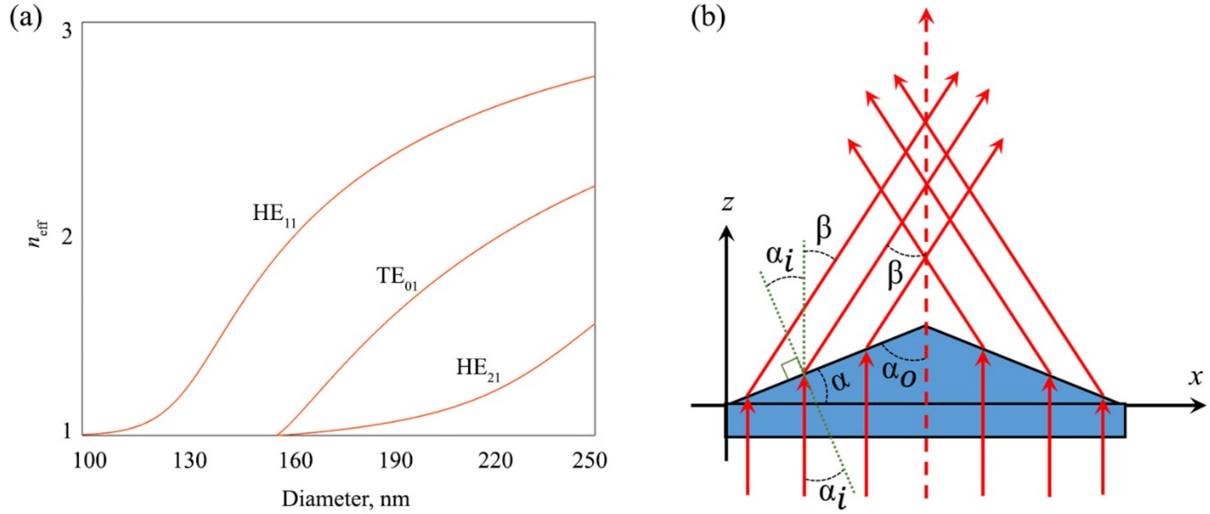

Figure S1. (a) Normalized propagation constant or effective refractive index as a function of diameter for some low order modes of an indexed-waveguide. (b) Working principle of conventional Axicon. A conventional axicon with angle α_0 is illuminated from the bottom with light source at incidence angle [illegible]$_i$.

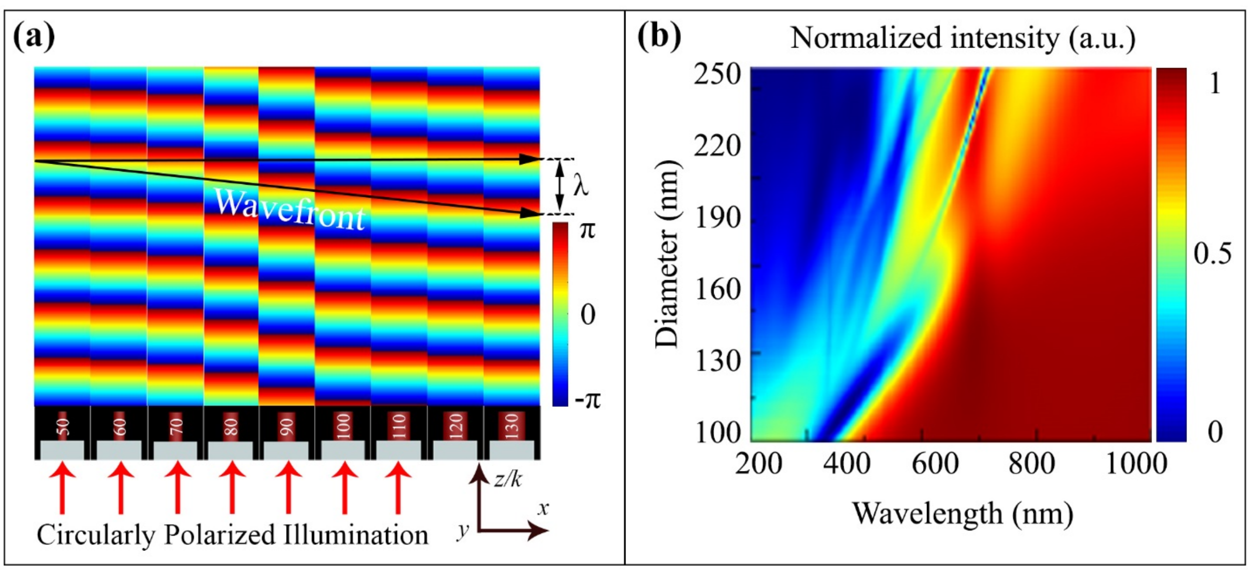

Figure S2. Phase profile under circularly polarized light and numerically simulated transmission amplitude for wavelength vs diameter.

Initial verification of the proposed meta-axicons also due to limited computational resources, a small portion (18 µm × 18 µm) of the designed metasurfaces with a lattice constant 300 nm is numerically simulated for topological charge m = 0, 2 and 4. Full-wave electromagnetic simulations are performed with perfectly matched layer (PML) boundary conditions in all directions. Each meta-axicon with different topological charge is numerically simulated for NA = 0.1, 0.7 and 0.9. A plane wave source with the operational wavelength of 633 nm is used to impinge the light on the meta-axicons from the substrate side. Cylindrical nano-resonators of a-Si:H with 400 nm thickness are tiled on a transparent glass substrate. The diffracted light from the array of nano-resonators is collected by monitors placed along the x-y and x-z planes respectively. Numerically simulated results of the all-dielectric meta-axicons under linear and circular polarization state of the incident light for topological charge m = 0, 2 and 4 are presented in Fig. S3. For NA = 0.1, Fig. S3a-f describe the behavior of meta-axicon with different topological charges while Fig. S3g-l represents the same behavior for NA = 0.9. Fig. S3a, c and e describe the transverse intensity distribution of the diffracted light captured by the x-y monitor possessing the doughnut shape intensity pattern accompanied with its longitudinal intensity profile captured by the x-z monitor. These results show the behavior of non-diffracting BB's, for topological charge m = 0, 2 and 4 respectively under linear polarization of the source. Fig. S3b, d and f illustrate the same behavior but under circularly polarized illumination.

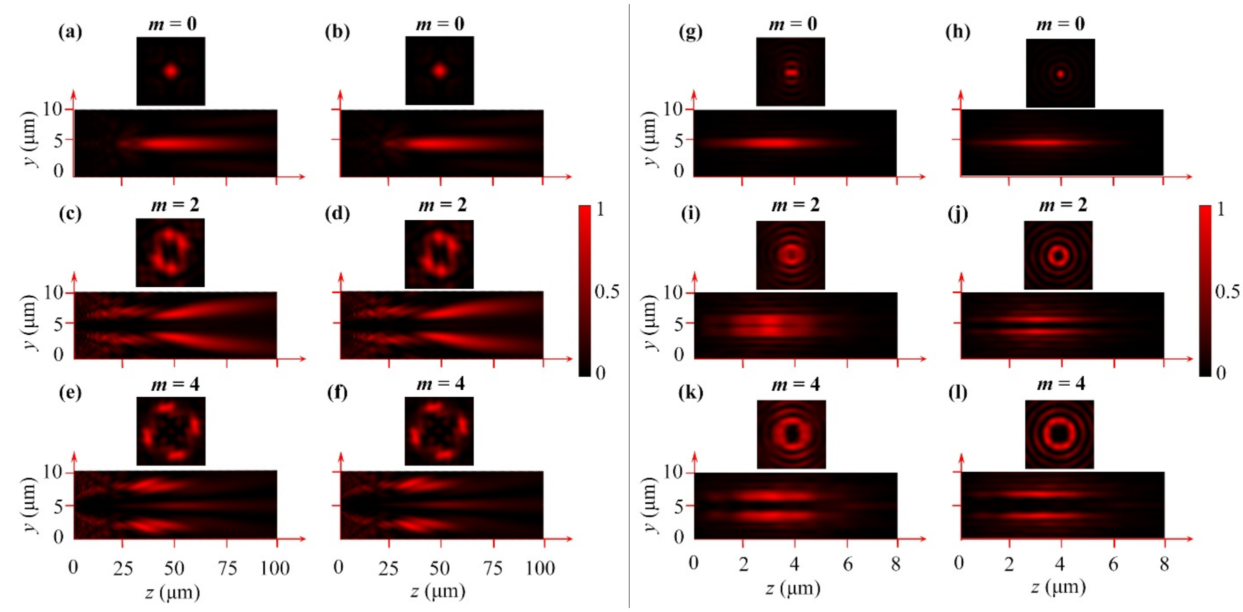

Figure S3. Numerically simulated results of the all-dielectric meta-axicons with different numerical apertures. (a-f) present the numerically simulated results for NA = 0.1 while (g-l) for NA = 0.9. (a), (c) and (e) represent the generation of non-diffracting twisted beams under linearly polarized plane wave for the topological charge of 0, 2 and 4. Transverse monitors placed along the x-y axis represents the intensity distribution while longitudinal monitor placed along the x-z axis show the non-diffracting behavior of the meta-axicons. (b), (d) and (f) represent the similar behavior but with the circularly polarized source. Therefore, as the topological charge increases, central defect or zero-intensity region and the helical phase fronts also increase.

A close inspection of the field distribution in Fig. S3 reveals that as topological charge increases from 0 to 4, the central defect along the direction of propagation increases and number of intertwined spirals also increases. Full-wave electromagnetic simulations demonstrate that high diffraction efficiency is observed in our meta-axicons where scattering performance of individual meta-axicon is determined by the constructive interference of the transmitted light. In conclusion, the proposed concept of polarization insensitive all-dielectric metasurfaces to generate non-diffracting twisted beams via meta-axicons is verified by having completely identical results under linear and circular polarization of the incident.

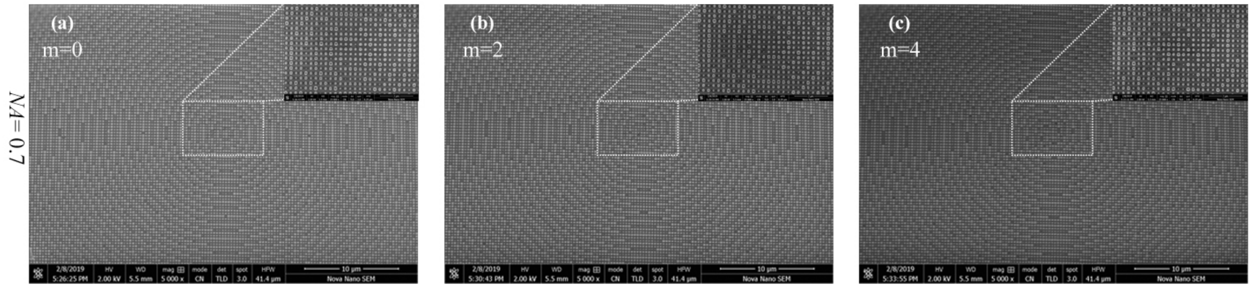

Figure S4. SEM images of the fabricated meta-axicons. (a-c) Illustrate the low magnification SEM images of the meta-a xicons with NA = 0.7 having topological charge m = 0, 2 and 4. The inset in each subfigure shows the high magnific ation version from the center of the each structure. The scale bar for low magnification images is 10 µm while for t he inset is 2 µm.

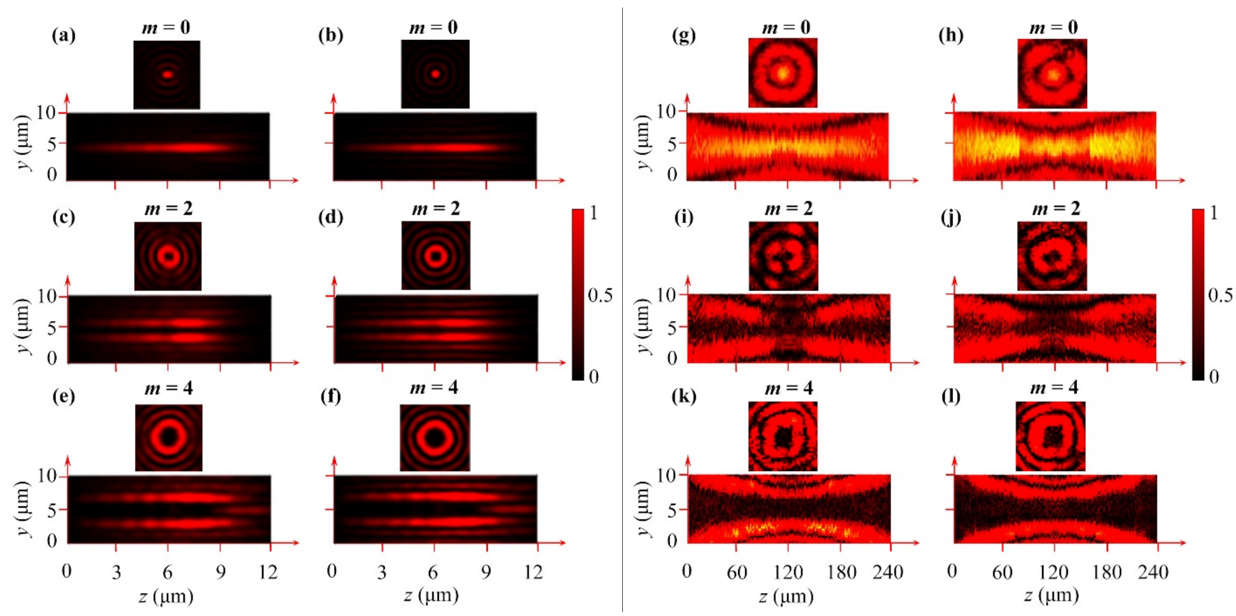

Figure S5. Numerically simulated results of the all-dielectric meta-axicons for numerical aperture NA=0.7. (a-f) present the numerically simulated results for NA = 0.7 while (g-l) represent the experimental results for generation of non-diffracting twisted beams under linearly polarized plane wave for the topological charge of 0, 2 and 4. Transverse monitors place d along the x-y axis represents the intensity distribution while longitudinal monitor placed along the x-z axis show the non-diffracting behavior of the meta-axicons.

We have also numerically verified the focusing performance of our meta-axicons, in terms of full width half maximum (FWHM), for the numerical apertures of 0.1, 0.7 and 0.9 as given in Fig. S6. The meta-axicon with the topological charge of m=0 is illuminated with circularly polarized plane wave source. The results for xy-plane and xz-plane intensity plots along with line-plots, depicting the FMWM, are represented in Fig. S6. It is found that FWHM of 3.579 λ, 0.511 λ, and 0.365 λ can be obtained for the numerical apertures of 0.1, 0.7 and 0.9 respectively. These analyses agree well with our expected results that the higher numerical aperture meta-axicons can give highly confined spot (without requiring an additional component) leading towards a subwavelength FWHM which is impossible to achieve from the conventional bulky axicons.

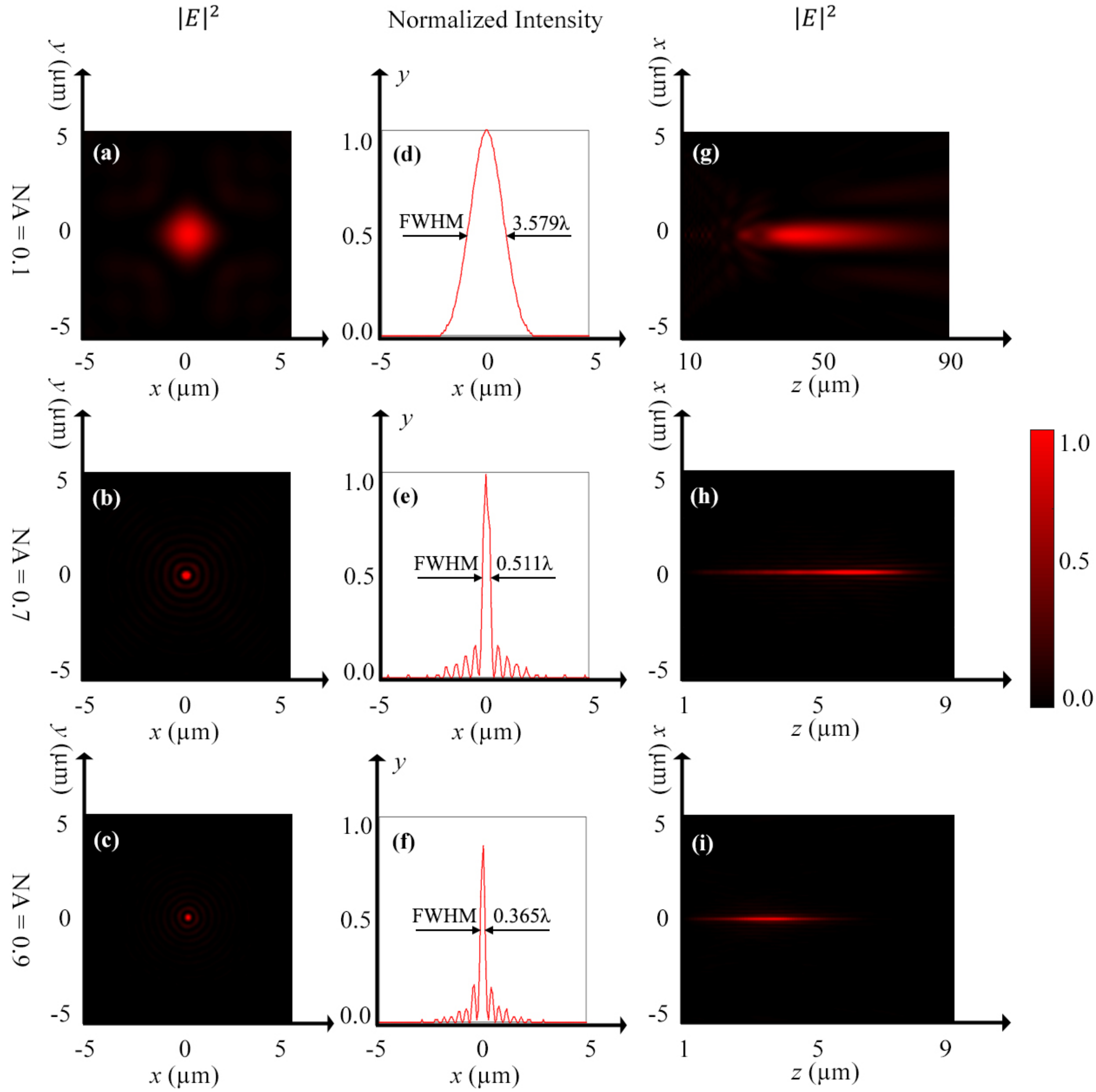

Figure S6. Numerically simulated full width half maximum of the zeroth order beam for NA = 0.1, 0.7 and 0.9. (a-c) describes the intensity profile at focal plane. (d-f) describe the FWHM while (g-i) illustrate the intensity profile along the direction of propagation. It is realized that metasurface-based structures can provide subwavelength spatial resolution ultimately resulting high numerical aperture and even smaller FWHM.